Nonlinear theory of classical cylindrical Richtmyer-Meshkov instability for arbitrary Atwood numbers

Wan Hai Liu, Chang Ping Yu, Wen Hua Ye, Li Feng Wang, and Xian Tu He

Citation: Physics of Plasmas (1994-present) **21**, 062119 (2014); doi: 10.1063/1.4883222
View online: http://dx.doi.org/10.1063/1.4883222
View Table of Contents: http://scitation.aip.org/content/aip/journal/pop/21/6?ver=pdfcov
Published by the AIP Publishing

Nonlinear theory of classical cylindrical Richtmyer-Meshkov instability for arbitrary Atwood numbers

Wan Hai Liu (刘万海),[1,2] Chang Ping Yu (于长平),[3,a)] Wen Hua Ye (叶文华),[2,4,5] Li Feng Wang (王立锋),[2,4] and Xian Tu He (贺贤土)[2,4]
[1]*Research Center of Computational Physics, Mianyang Normal University, Mianyang 621000, China*
[2]*HEDPS and CAPT, Peking University, Beijing 100871, China*
[3]*LHD, Institute of Mechanics, Chinese Academy of Sciences, Beijing 100190, China*
[4]*Institute of Applied Physics and Computational Mathematics, Beijing 100094, China*
[5]*Department of Physics, Zhejiang University, Hangzhou 310027*

(Received 31 March 2014; accepted 2 June 2014; published online 27 June 2014)

A nonlinear theory is developed to describe the cylindrical Richtmyer-Meshkov instability (RMI) of an impulsively accelerated interface between incompressible fluids, which is based on both a technique of Padé approximation and an approach of perturbation expansion directly on the perturbed interface rather than the unperturbed interface. When cylindrical effect vanishes (i.e., in the large initial radius of the interface), our explicit results reproduce those [Q. Zhang and S.-I. Sohn, Phys. Fluids 9, 1106 (1996)] related to the planar RMI. The present prediction in agreement with previous simulations [C. Matsuoka and K. Nishihara, Phys. Rev. E **73**, 055304(R) (2006)] leads us to better understand the cylindrical RMI at arbitrary Atwood numbers for the whole nonlinear regime. The asymptotic growth rate of the cylindrical interface finger (bubble or spike) tends to its initial value or zero, depending upon mode number of the initial cylindrical interface and Atwood number. The explicit conditions, directly affecting asymptotic behavior of the cylindrical interface finger, are investigated in this paper. This theory allows a straightforward extension to other nonlinear problems related closely to an instable interface. © *2014 AIP Publishing LLC*. [http://dx.doi.org/10.1063/1.4883222]

I. INTRODUCTION

When an incident shock collides with a corrugated interface separating two fluids of different densities, the interface is with Richtmyer-Meshkov instability (RMI).[1,2] Another wide class of RMI, not related to the shock-interface interaction, is driven by the nonuniform vorticity on the interface, either initially deposited or supplied by external sources.[3] RMI has great relevance to inertial confinement fusion (ICF) and astrophysical problems.[4,5]

As the incident shock collides with the material interface, it bifurcates into a transmitted shock and a reflected wave. The reflected wave can be either a shock wave or a rarefaction wave, which depends on the material properties of the fluids across the interface and the incident shock strength. When the shock collides with the material interface from the light fluid phase to the heavy fluid phase, the reflected wave is a shock; otherwise, it is a rarefaction wave. See Ref. 6 for further details of the reflected wave types. For the case of the reflected shock, the perturbed interface grows linearly at first, and then exhibits in the shapes of bubbles, and spikes in its weakly nonlinear regime. The bubbles (spikes) refer to the portions of the light (heavy) fluid entering the heavy (light) fluid. For this case, the fluids near the material interface can be approximated to be incompressible after both the transmitted shock and reflected one depart from the interface.

Some experiments[7–9] and numerical simulations[10–15] on the growth rate of the RMI interface have been performed, and several theories[16–22] have been predicted by different approaches. Most of these theoretical literatures just concerned with the linear growth rate of the interface at earlier stage. For several decades, theories could not give a quantitatively correct prediction for the growth rate of RMI interface in the nonlinear regime until Zhang's nonlinear theory[23] was published. The theory provided a pretty result for the planar RMI interface. The prediction of this theory, based on the case of a reflected wave, is in excellent agreement with the results of full nonlinear numerical simulations, and with experimental data from the earlier linear stage to the later nonlinear stage. In this theory, the perturbation solutions in weakly nonlinear regime led to a perfect Padé approximation which gave the final result by matching the linear solution and the asymptotic solution. In addition, Velikovich and Dimonte[24] successfully investigated the incompressible RMI by using the Padé approximation based on nonlinear perturbation theory.

Most previous works focused on the planar RMI, however, only a few[3,24–29] dealt with the cylindrical RMI which is much closer to the applications, such as ICF. For cylindrical RMI, scaling laws for unstable interfaces driven by strong shocks were researched numerically.[27] The effect of convergence on the interface growth rate was studied experimentally on the OMEGA laser.[28] In Ref. 29, the dependence of growth rates of a bubble and spike on the fluid densities and on mode number involved in the initial perturbations was seeded analytically by employing the method used in the investigation.[23] A crucial step of the method is based on the fact that the physical quantities on the perturbed interface are expanded into Taylor series indirectly on the unperturbed interface. This step is considerably complex, especially to the cylindrical system. In this paper, for the case of the reflected shock, we employ a simple

[a)]Author to whom correspondence should be addressed. Electronic mail: champion-yu@163.com

method based directly on the perturbed interface to solve the cylindrical RMI problem in weakly nonlinear regime by considering the nonlinear correction up to fourth order. Applying the technique of the Padé approximation results in the growth rates of the interface fingers for the whole nonlinear regime.

II. THEORETICAL FRAMEWORK AND EXPLICIT RESULTS

Our insight starts from the time when the reflected and transmitted shocks leave the interface and the fluids in the vicinity of the interface can be regarded as impressible ones. In the cylindrical geometry (r, θ, z), the initial interface is given to be located at

$$r = a(\theta, t=0) = r_0 + a_0\cos(n\theta), \tag{1}$$

where $n = 2\pi r_0/\lambda$ is mode number, r_0 is the initial radius of the interface, λ is perturbation wavelength, and a_0 is the perturbation amplitude of the interface ($a_0 \ll \min\{\lambda, r_0\}$). The initial velocity distribution of the interface is

$$\left.\frac{\partial a(\theta,t)}{\partial t}\right|_{t=0} = v_0\cos(n\theta), \tag{2}$$

where v_0 is proportional to a_0 in the magnitude. The interface $a(\theta, t)$, due to the cylindrical RMI, evolves with time. It is dominated by

$$\frac{\partial}{\partial r}\left(r\frac{\partial\phi_i}{\partial r}\right) + \frac{\partial}{\partial\theta}\left(\frac{1}{r}\frac{\partial\phi_i}{\partial\theta}\right) = 0 \qquad \text{in two fluids,} \tag{3a}$$

$$\frac{\partial a}{\partial t} + \frac{1}{r^2}\frac{\partial a}{\partial\theta}\frac{\partial\phi_1}{\partial\theta} - \frac{\partial\phi_1}{\partial r} = 0 \qquad \text{at} \quad r = a(\theta,t), \tag{3b}$$

$$\frac{\partial a}{\partial t} + \frac{1}{r^2}\frac{\partial a}{\partial\theta}\frac{\partial\phi_2}{\partial\theta} - \frac{\partial\phi_2}{\partial r} = 0 \qquad \text{at} \quad r = a(\theta,t), \tag{3c}$$

$$\begin{aligned}&(1+A)\left[\frac{\partial\phi_1}{\partial t} + \frac{1}{2}\left(\frac{\partial\phi_1}{\partial r}\right)^2 + \frac{1}{2r^2}\left(\frac{\partial\phi_1}{\partial\theta}\right)^2\right]\\ &-(1-A)\left[\frac{\partial\phi_2}{\partial t} + \frac{1}{2}\left(\frac{\partial\phi_2}{\partial r}\right)^2 + \frac{1}{2r^2}\left(\frac{\partial\phi_2}{\partial\theta}\right)^2\right]\\ &+f(t) = 0 \qquad \text{at} \quad r = a(\theta,t),\end{aligned} \tag{3d}$$

where Atwood number $A = (\rho_1 - \rho_2)/(\rho_1 + \rho_2)$ with ρ_1 and ρ_2 being fluid densities, and ϕ_i is velocity potential function of the fluid, and $f(t)$ is an arbitrary function of time. Throughout this paper, we determine the subscripts 1 and 2 corresponding to the physical quantities at the inner and outer regions of the interface, respectively. Accordingly, $A > 0$ corresponds to a case of an incident shock traveling from the lighter fluid outsider the interface to the heavy one insider the interface, and $A < 0$ means a case of an incident shock advancing from the lighter fluid insider the interface to the heavy fluid outsider the interface.

The interface and velocity potentials at time t can be expressed as

$$\begin{aligned}a(\theta,t) = \zeta(t)r_0 + \sum_{l=1}^{L} a^{(l)}(\theta,t) = r_0\left(1 + \sum_{l=1}^{\lfloor\frac{L}{2}\rfloor}\varepsilon^{2l}a_{2l,0}(t)\right)\\ + \sum_{l=1}^{L}\varepsilon^l\sum_{m=0}^{\lfloor\frac{l}{2}\rfloor-1} a_{l,l-2m}(t)\cos(l-2m)n\theta + O(\varepsilon^{L+1}),\end{aligned} \tag{4a}$$

$$\begin{aligned}\phi_1(r,\theta,t) = \sum_{l=1}^{L}\phi_1^{(l)}(r,\theta,t) = \sum_{l=1}^{L}\varepsilon^l\sum_{m=0}^{\lfloor\frac{l}{2}\rfloor}\phi_{1,l,l-2m}(t)r^{(l-2m)n}\\ \times\cos(l-2m)n\theta + O(\varepsilon^{L+1}),\end{aligned} \tag{4b}$$

$$\begin{aligned}\phi_2(r,\theta,t) = \sum_{l=1}^{L}\phi_2^{(l)}(r,\theta,t) = \sum_{l=1}^{L}\varepsilon^l\sum_{m=0}^{\lfloor\frac{l}{2}\rfloor}\phi_{2,l,l-2m}(t)r^{-(l-2m)n}\\ \times\cos(l-2m)n\theta + O(\varepsilon^{L+1}),\end{aligned} \tag{4c}$$

where the parameter $\varepsilon = a_0/\kappa$ with $\kappa = \min\{r_0, \lambda\}$ is much less than 1 and $L = 4$ is selected. Gauss symbol $\lfloor l/2\rfloor$ denotes the maximum integer which is less than or equal to $l/2$. The time function $\zeta(t)$ determines whether the unperturbed interface moves with time: the interface will keep resting when $\zeta(t) \equiv 1$; otherwise, it will move from the initial position r $(t=0) = r_0$. Unknowns $a_{l,l-2m}(t)$, $\phi_{1,l,l-2m}(t)$, and $\phi_{2,l,l-2m}(t)$ $[l = 1, 2, \cdots; m = 0, 1, \cdots, \lfloor l/2\rfloor]$ always need to be ascertained. Note that velocity potentials $\phi_1(r,\theta,t)$ and $\phi_2(r,\theta,t)$ have satisfied the Laplace equation (3a) and conditions $\nabla\phi_1(r,\theta,t)|_{r\to 0} = 0$ and $\nabla\phi_2(r,\theta,t)|_{r\to+\infty} = 0$.

We substitute Eqs. (4a)–(4c) into Eqs. (3b)–(3d) and then replace r in these three resulting equations with $a(\theta, t)$ expressed by Eq. (4a). The final equations containing θ and ε are obtained. To further obtain the lth $(l > 0)$ order equations just including the terms of ε^l, we need to expand the left hand sides of these three final equations in Maclaurin series of ε. Here, the zeroth order equations, considering the effect of arbitrary function $f(t)$, can be satisfied automatically. Therefore, the first-, second-, third-, and fourth-order equations together with the initial conditions (1) and (2) can be solved successively.

The results related to perturbed interface are

$$a^{(1)} = (a_0 + tv_0)\cos(n\theta), \tag{5a}$$

$$a^{(2)} = \frac{t^2v_0^2(2An-1)}{4r_0}\cos(2n\theta) - \frac{tv_0(2a_0+tv_0)}{4r_0}, \tag{5b}$$

$$\begin{aligned}a^{(3)} = &\frac{t^2v_0^2\left[a_0(-2An-3n^2+1) + tv_0(4A^2n^2-4An-n^2+1)\right]}{8r_0^2}\cos(3n\theta)\\ &-\frac{t^2v_0^2\left[3a_0(2An+n^2-7) + tv_0(4A^2n^2+4An+n^2-9)\right]}{24r_0^2}\cos(n\theta),\end{aligned} \tag{5c}$$

$$a^{(4)} = \frac{\alpha t^2 v_0^2}{192 r_0^3}\cos(4n\theta) - \frac{\beta t^2 v_0^2}{48 r_0^3}\cos(2n\theta) + \frac{\gamma t^2 v_0^2}{192 r_0^3}, \tag{5d}$$

where

$$\alpha = -8ta_0v_0\left[14A^2n^2 + A(16n^2-13)n - 14n^2 + 3\right] + 12a_0^2 \times \left[2A(2n^3+n) + 7n^2 - 1\right] + t^2v_0^2(128A^3n^3 - 188A^2n^2 - 64An^3 + 92An + 44n^2 - 15),$$

$$\beta = 2ta_0v_0[4A^2n^2 - 24An - 16n^2 + 21] + 12a_0^2[A(n^3+n) - 3n^2 + 2] + t^2v_0^2(16A^3n^3 - 4A^2n^2 - 22An - 8n^2 + 15),$$

and

$$\gamma = 8ta_0v_0[2(A^2+1)n^2 + 5An - 18] + 12a_0^2(2An + n^2 - 9) + t^2v_0^2[4n(A^2n + 7A + n) - 45].$$

Taking wave number $k = 2\pi/\lambda$ and mode number $n = 2\pi r_0/\lambda$ into account, one obtains $n = kr_0$. Replacing n in Eqs. (5a)–(5d) with kr_0, and taking the limit $r_0 \to +\infty$, the results corresponding to the planar geometry predicted by Ref. 23 are reproduced. That is, in the condition of large r_0, the cylindrical RMI problem is reduced to the planar one.

III. PADÉ APPROXIMATION AND DISCUSSION

To probe into growth rates of spikes and bubbles for $A > 0$ case, we select a spike located at $\theta = 0$ and a bubble at $\theta = \pi/n$. Letting v_{sp} and v_{bb} denote the growth rates at the tips of spike and bubble, respectively, one has

$$v_{sp} = \dot{a}_o(0,t) + \dot{a}_e(0,t), \tag{6a}$$

$$v_{bb} = -\dot{a}_o(0,t) + \dot{a}_e(0,t), \tag{6b}$$

where the dot over a letter denotes the time derivative. The a_o and a_e result from odd and even (including the nonoscillation terms, i.e., zeroth harmonic) cosine Fourier modes, respectively. The $\dot{a}_o$ represents the overall growth rate defined as

$$v_{overall} = (v_{sp} - v_{bb})/2 = (\dot{r}_{max} - \dot{r}_{min})/2, \tag{7}$$

and $\dot{a}_e$ means $(v_{sp} + v_{bb})/2$. They are

$$\dot{a}_o(0,t) \approx v_0 + \frac{\left(-Ana_0v_0^2 - n^2a_0v_0^2 + 2a_0v_0^2\right)}{r_0^2}t + \frac{\left(2A^2n^2v_0^3 - 4Anv_0^3 - n^2v_0^3 + 3v_0^3\right)}{2r_0^2}t^2, \tag{8a}$$

$$\dot{a}_e(0,t) \approx -\frac{a_0v_0}{2r_0} + \frac{v_0^2\left[a_0^2(10n^2-9) + 4r_0^2(An-1)\right]}{4r_0^3}t - \frac{a_0v_0^3[8A^2n^2 + A(8n^2-21)n - 16n^2 + 21]}{4r_0^3}t^2 + \frac{v_0^4(8A^3n^3 - 21A^2n^2 - 8An^3 + 26An + 10n^2 - 15)}{6r_0^3}t^3. \tag{8b}$$

As is well known, above solutions can just serve to describe the interface movement in the weakly nonlinear regime. For the stage of the nonlinear regime prior to turbulent mixing, these weakly nonlinear solutions fail to play a correct role. One of the standard methods to extend the range of validity beyond the range of the finite Taylor series expansion is a Padé approximation.[23,24,30,31] Applying the Padé to Eq. (8a), one has

$$\dot{a}_o(0,t) = \frac{v_0}{1 + \frac{a_0v_0(An+n^2-2)}{r_0^2}t + \max\left\{0, \frac{2a_0^2(An+n^2-2)^2 + r_0^2(-2A^2n^2 + 4An + n^2 - 3)}{2r_0^4}\right\}v_0^2t^2}. \tag{9}$$

Equation (9) is selected as P_2^0 or P_1^0 Padé approximation according to the fact that the overall growth rate decays at large times predicted in Ref. 3. For Eq. (8b), the P_2^1 Padé approximation is constructed as

$$\dot{a}_e(0,t) = \frac{\varsigma v_0 + \tau v_0^2 t}{4r_0^3\left(\xi + \varrho a_0v_0t + \chi v_0^2t^2\right)}, \tag{10}$$

where

$$\varsigma = 12a_0^3r_0^4(8A^2n^2 - 32An^3 + 15An + 24n^2 - 15) - 96a_0r_0^6(An-1)^2 - 6a_0^5(9-10n^2)^2r_0^2,$$

$$\begin{aligned}\tau = {} & 24a_0^4r_0^2(10n^2-9)\left[-4A^2n^2 + A(11n^2-3)n - 7n^2 + 3\right] \\ & - 8a_0^2r_0^4\left[40A^3n^3 + A^2(9n^2 - 132n^4) + 14A(16n^2-7)n - 94n^2 + 51\right] \\ & + 3a_0^6(10n^2-9)^3 + 192r_0^6(An-1)^3,\end{aligned}$$

$$\xi = -6a_0^2r_0^2(8A^2n^2 - 32An^3 + 15An + 24n^2 - 15) + 3a_0^4(9-10n^2)^2 + 48r_0^4(An-1)^2,$$

$$\begin{aligned}\varrho = {} & 3a_0^2(10n^2-9)\left[8A^2n^2 + A(8n^2-21)n - 16n^2 + 21\right] \\ & + 8r_0^2\left[8A^3n^3 + 3A^2(4n^2-11)n^2 + A(50n - 32n^3) + 19n^2 - 24\right],\end{aligned}$$

and

$$\begin{aligned}\chi = {} & a_0^2\left[192A^4n^4 + 32A^3(7n^2-27)n^3 + 3A^2(64n^4 - 452n^2 + 651)n^2\right] \\ & + Aa_0^2[(-608n^5 + 2360n^3 - 2178n) + 568n^4 - 1536n^2 + 1053] \\ & - 8r_0^2\left[8A^4n^4 - 29A^3n^3 + A^2(47n^2 - 8n^4) + A(18n^2-41)n - 10n^2 + 15\right].\end{aligned}$$

It is worth noting that the expressions of Padé (9) and (10) obtained for the cylindrical geometry can be reduced to Eqs. (53) and (54)[23] when $n = kr_0$ and in the limit of large r_0. Thus, the growth rates of the spike tip (6a), bubble tip (6b), and the overall interface (7) based on Padé approximations (9) and (10) are formulated for $A > 0$ case. For $A < 0$ case, the positions of a bubble and a spike need to be exchanged each other. In addition, based on the singularity of Padé approximation, Eqs. (9) and (10) are available for the physical parameter space $n^2 + An - 2 > 0$, $\varrho/\xi > 0$, and $\chi/\xi > 0$ with $\xi \neq 0$.

In fact, when a_0 is much smaller than λ or r_0, the fully nonlinear evolution of the interface does not much depend on the initial amplitude a_0.[32] As a result, under the condition $a_0 = 0$, expressions (9) and (10) normalized by r_0 and v_0 can be reduced to

$$\dot{\hat{a}}_o(0,\hat{t}) = \frac{1}{1 + \max\left\{0, -\frac{1}{2}(2A^2n^2 - 4An - n^2 + 3)\right\}\hat{t}^2}, \tag{11a}$$

$$\dot{\hat{a}}_e(0,\hat{t}) = \frac{(An-1)\hat{t}}{1 + \dfrac{8A^3n^3 - 21A^2n^2 - 8An^3 + 26An + 10n^2 - 15}{6(1-An)}\hat{t}^2}, \tag{11b}$$

where symbol ˆ denotes the normalized physical quantity.

To confirm the validity of the theoretical prediction, we show the normalized growth rates of the bubble and spike against normalized time at $A = -0.2$ [$A = 0.2$] for variable mode numbers in Fig. 1(i) [Fig. 1(ii)]. The corresponding growth rates with the same mode numbers as ours can be seen in Figs. 2(a)–2(d) in Matsuoka's simulation work,[3] where $A = \pm 0.2$ corresponds to $A = \mp 0.2$ of this paper. Their Figs. 2(a)–2(d), based on a nonphysical parameter $\delta = 0$ for $n = 1$ and $\delta = 0.1$ for other mode numbers, show the growth rates at early times and at fully nonlinear stage, respectively. Note that, in their Figs. 2(a) and 2(b), only the partial curves of the growth rates are plotted before the calculations break down. These factors result in the

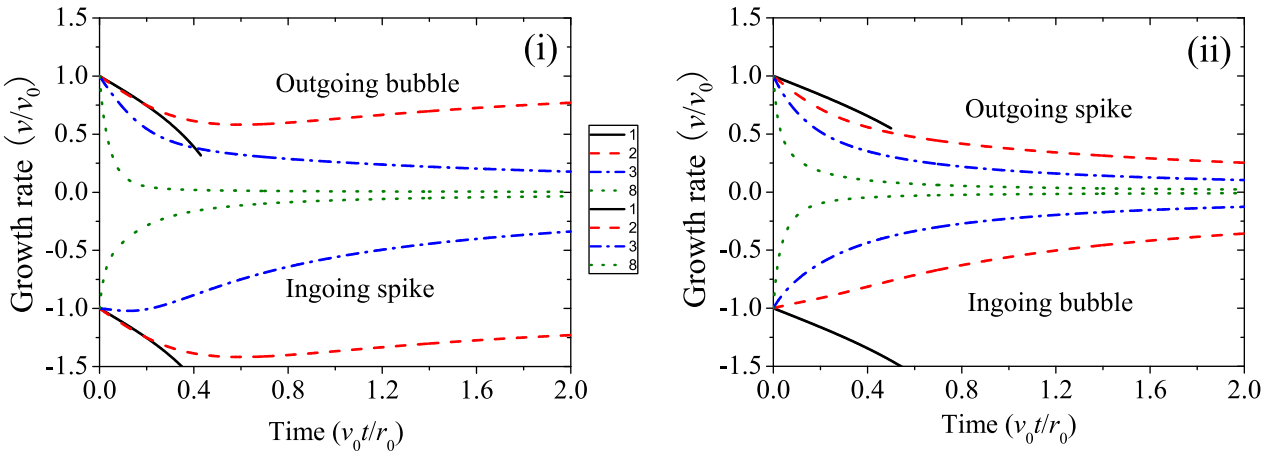

FIG. 1. Normalized growth rates of bubble and spike, v_{bb}/v_0 and v_{sp}/v_0, vs normalized time, v_0t/r_0, at $A = -0.2$ (i) and $A = 0.2$ (ii). Different mode numbers $n = 1$, 2, 3, and 8 are, separately, denoted by lines, dashed lines, dotted-dashed lines, and dotted lines. The initial perturbation amplitude is fixed as $a_0/r_0 = 0$.

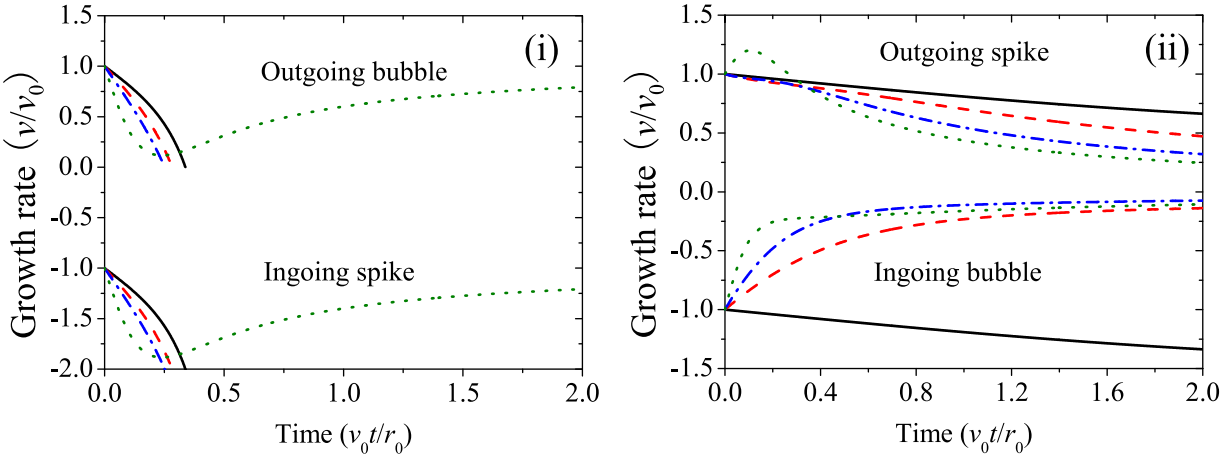

FIG. 2. Normalized growth rates of bubble and spike, v_{bb}/v_0 and v_{sp}/v_0, vs normalized time, v_0t/r_0, at $A=-0.8$ (i) and $A=0.8$ (ii). Different mode numbers $n=1$, 2, 3, and 8 are, separately, denoted by lines, dashed lines, dotted-dashed lines, and dotted lines. The initial perturbation amplitude is fixed as $a_0/r_0=0$.

small difference between their Figs. 2(a) and 2(c) [Figs. 2(b) and 2(d)] and Fig. 1(i) [Fig. 1(ii)] in this paper. However, the trends of the growth rates of the bubble and spike are the same.

Figure 1 shows that for smaller Atwood number (i.e., $A=\pm0.2$), the normalized growth rate v/v_0 of outgoing bubble (spike) or ingoing spike (bubble) tends to different values with time, depending on mode number. When mode number is larger, the v/v_0 of the bubble and spike approaches zero. The larger the mode number is, the faster the v/v_0 reaches zero. For the smaller mode number (e.g., $n=1$), the movement of outgoing bubble (spike) becomes slowly with time, while the ingoing spike (bubble) accelerates its speed toward to the center of the inner fluid. It is evident that mode number directly influences the evolution behavior of the bubble and spike.

To seek effect of Atwood number on the bubble and spike, we show the v/v_0 of bubble and spike for $A=\pm0.8$ with normalized time in Fig. 2. Atwood number has a dramatic influence on the evolution of the bubble and spike, especially on outgoing bubble and ingoing spike in Fig. 2(i),

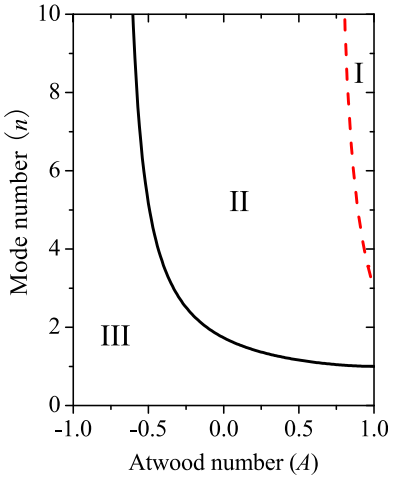

FIG. 3. Parameter space: region II corresponds to $2A^2n^2-4An-n^2+3<0$; regions I and III correspond to $2A^2n^2-4An-n^2+3\geq0$.

where the v/v_0 does not tend to zero for mode number $n=1$, 2, 3, or 8. As a result, it is necessary to investigate asymptotic behavior of the bubble and spike. From expressions (11a) and (11b), we have

$$\dot{\hat{a}}_o(0,\hat{t}\to+\infty)=\begin{cases}0, & 2A^2n^2-4An-n^2+3<0,\\ 1, & \text{otherwise.}\end{cases} \tag{12a}$$

$$\dot{\hat{a}}_e(0,\hat{t}\to+\infty)=0. \tag{12b}$$

In accordance with growth rates (6a) and (6b), we can get

$$\hat{v}_{sp}(\hat{t}\to+\infty)=\begin{cases}0, & 2A^2n^2-4An-n^2+3<0,\\ 1, & \text{otherwise,}\end{cases} \tag{13}$$

and

$$\hat{v}_{bb}(\hat{t}\to+\infty)=\begin{cases}0, & 2A^2n^2-4An-n^2+3<0,\\ -1, & \text{otherwise.}\end{cases} \tag{14}$$

These expressions show that for the case of $2A^2n^2-4An-n^2+3<0$, the normalized asymptotic growth rates of outgoing spike and ingoing bubble are both zero; otherwise, they, respectively, tend to 1 and -1. Relationship $2A^2n^2-4An-n^2+3<0$ means mode number n between $A_c^{(1)}$ and $A_c^{(2)}$, in which $A_c^{(1)}=\left(2A+\sqrt{3-2A^2}\right)/\left(2A^2-1\right)$ and $A_c^{(2)}=\left(2A-\sqrt{3-2A^2}\right)/\left(2A^2-1\right)$. That is to say, when mode number is between $A_c^{(1)}$ and $A_c^{(2)}$ corresponding to region II shown in Fig. 3, the asymptotic growth rate of neither outgoing (ingoing) bubble or ingoing (outgoing) spike tends to rest; otherwise (i.e., regions I and III shown in Fig. 3), it does to its initial value. Especially for the ingoing spike, shown in Figs. 1(i) and 2(i), the asymptotic growth rate profoundly influences the time evolution of the spike. For calculation simulations, the prompt acceleration of ingoing spike directly makes the calculation break down easily.

IV. CONCLUSION

In summary, we apply an approach of the perturbation expansion to explore the problem of cylindrical RMI in incompressible, inviscid, and irrotational fluids directly at the perturbed interface rather than the unperturbed one and obtain the explicit solutions up to the fourth order in the weakly nonlinear regime. Padé approximation employed in the perturbation solutions results in the nonlinear results which are valid for the full nonlinear regime before turbulence mixing. In the limit of large initial interface radius, our results reproduce the previous work[23] which is extremely valid for the planar case. Comparison between the fully nonlinear simulation from Matsuoka and Nishihara[3] and our explicit prediction is manipulated, and the qualitative agreement denotes that the theoretical results are helpful to better understand cylindrical RMI. The asymptotic growth rate of outgoing bubble (spike) or ingoing spike (bubble) tends to either its initial velocity or zero, depending on mode number and Atwood number. This theory provided here allows a straightforward extension to other nonlinear problems related closely to an instable interface.

ACKNOWLEDGMENTS

The author Liu sincerely thanks the anonymous reviewer for the valuable comments that have led to the present improved version of the original manuscript. This work was supported by the National Natural Science Foundation of China (Grant Nos. 11275031, 10835003, 11372330, 11072248, and 11274026), the 863 Program (No. 2012AA01A304), the CAS Program (Nos. KJCX2-EW-J01, XXH12503-02-02-04) and the National High-Tech ICF Committee.

[1]R. D. Richtmyer, Commun. Pure Appl. Math. **13**, 297, (1960).
[2]E. E. Meshkov, Fluid Dyn. **4**, 101 (1969).
[3]C. Matsuoka and K. Nishihara, Phys. Rev. E **73**, 055304(R) (2006).
[4]B. A. Remington, J. Kane, R. P. Drake, S. G. Glendinning, K. Estabrook, R. London, J. Castor, R. J. Wallace, D. Arnett, E. Liang, R. McCray, A. Rubenchik, and B. Fryxell, Phys. Plasmas **4**, 1994 (1997).
[5]S. W. Haan, Phys. Plasmas **2**, 2480 (1995).
[6]Y. Yang, Q. Zhang, and D. H. Sharp, Phys. Fluids **6**, 1856 (1994).
[7]A. N. Aleshin, E. V. Lazareva, S. G. Zaitsev, V. B. Rozanov, E. G. Gamali, and I. G. Lebo, Sov. Phys. Dokl. **35**, 159 (1990).
[8]R. Benjamin, D. Besnard, and J. Haas, LANL Report LA-UR 92-1185 (1993).
[9]G. Dimonte, Phys. Plasmas **6**, 2009 (1999).
[10]D. Oron, L. Arazi, D. Kartoon, A. Rikanati, U. Alon, and D. Shvarts, Phys. Plasmas **8**, 2883 (2001).
[11]J. W. Grove, R. Holmes, D. H. Sharp, Y. Yang, and Q. Zhang, Phys. Rev. Lett. **71**, 3473 (1993).
[12]K. O. Mikaelian, Phys. Rev. Lett. **71**, 2903 (1993).
[13]R. L. Holmes, J. W. Grove, and D. H. Sharp, J. Fluid Mech. **301**, 51 (1995).
[14]U. Alon, J. Hecht, D. Ofer, and D. Shvarts, Phys. Rev. Lett. **74**, 534 (1995).
[15]S.-I. Sohn, Phys. Rev. E **69**, 036703 (2004).
[16]S. W. Haan, Phys. Fluids B **3**, 2349 (1991).
[17]J. Hecht, U. Alon, and D. Shvarts, Phys. Fluids A **6**, 4019 (1994).
[18]Q. Zhang and S.-I. Sohn, Phys. Lett. A **212**, 149 (1996).
[19]S.-I. Sohn, Phys. Rev. E **67**, 026301 (2003).
[20]J. G. Wouchuk, Phys. Rev. E **63**, 056303 (2001).
[21]C. Mügler and S. Gauthier, Phys. Rev. E **58**, 4548 (1998).
[22]A. Rikanati, U. Alon, and D. Shvarts, Phys. Rev. E **58**, 7410 (1998).
[23]Q. Zhang and S.-I. Sohn, Phys. Fluids **9**, 1106 (1997).
[24]A. L. Velikovich and G. Dimonte, Phys. Rev. Lett. **76**, 3112 (1996).
[25]W. H. Liu, X. T. He, and C. P. Yu, Phys. Plasmas **19**, 072108 (2012).
[26]J. G. Wouchuk and K. Nishihara, Phys. Plasmas **4**, 1028 (1997).
[27]Q. Zhang and M. J. Graham, Phys. Rev. Lett. **79**, 2674 (1997).
[28]J. R. Fincke, N. E. Lanier, S. H. Batha, R. M. Hueckstaedt, G. R. Magelssen, S. D. Rothman, K. W. Parker, and C. J. Horsfield, Laser Part. Beams **23**, 21 (2005).
[29]C. Matsuoka and K. Nishihara, Phys. Rev. E **74**, 066303 (2006).
[30]A. Pozzi, *Applications of Padé Approximation Theory in Fluid Dynamics* (World Scientific, Singapore, 1994).
[31]C. M. Bender and S. A. Orszag, *Advanced Mathematical Methods for Scientists and Engineers* (McGraw-Hill, New York, 1978).
[32]C. Matsuoka and K. Nishihara, Phys. Rev. E **73**, 026304 (2006).